Applicability of Vertically Integrated Models for Carbon Storage Modeling in Structured Heterogeneous Domains

Karl W. Bandilla*, Bo Guo, Michael A. Celia

Department of Civil and Environmental Engineering, Princeton University, Princeton, NJ USA

Abstract

Numerical modeling is an essential tool for investigating the potential of geologic carbon storage and evaluating storage sites. Many different modeling approaches can be applied to problems related to geologic carbon storage, with the choice of modeling approach usually based the type of questions being asked, available computational resources and familiarity with the approach. One option is the vertically-integrated modeling approach, where the three-dimensional governing equations of multiphase flow are integrated over the thickness of the formation. In this paper, we present initial results of a study investigating the applicability of vertically-integrated models for CO_2 and brine migration in the context of geologic carbon storage in heterogeneous domains. Results from a full three-dimensional model are compared to results from a vertically-integrated simulator for two test cases. One test case consists of a horizontally homogeneous, but vertically heterogeneous domain (i.e., a layered domain). The second test case has two intersecting vertically heterogeneous channels imbedded in a homogeneous background. The results show good agreement between the two approaches for both the depth-average CO_2 plume outline, as well as for the predicted vertical CO_2 saturation profiles. Overall, the results suggest that vertically-integrated modeling may be applicable for domains with vertical heterogeneity, such as formation created in fluvial deposition environments.

1. Introduction

Carbon capture and storage (CCS) is a climate change mitigation technology in which carbon dioxide (CO_2) is captured at stationary CO_2 sources (e.g., fossil-fuel power plants, oil and gas processing plants) and injected into the

* Corresponding author. Tel.: +1-716-907-2540.
  E-mail address: bandilla@princeton.edu

deep subsurface [1, 2]. While several types of storage formations have been explored (e.g., depleted oil and gas fields, unminable coal seams), deep saline aquifers are considered the most favorable target for geologic carbon storage (GCS). As CO_2 is being injected into a saline aquifer it displaces the resident brine which either migrates laterally in the injection formation or vertically to over- and under-lying formations. CO_2 is usually injected at high enough pressure and temperature for it to be in its super-critical state. However, the density of the injected CO_2 is still between 250-750 kg/m^3 lower than the density of resident brine, leading to a strong vertical buoyant drive for CO_2. Therefore, a formation with low permeability (termed caprock) above the injection formation is necessary to prevent CO_2 from migrating upwards to shallower formations and the atmosphere. Even with an otherwise competent caprock, imperfections in the caprock, such as faults and abandoned wells, may allow for CO_2 leakage out of the injection formation. This leakage not only endangers the goal of safe and permanent storage of CO_2, but it may also impair overlying sources of drinking water through acidification and the subsequent release of otherwise immobile heavy metals. Brine may also migrate along caprock imperfection, endangering overlying drinking water resources by the transport of high salinity and potentially other contaminants. Along with the risks associated with CO_2 and brine migration, the injection induced pressure increase in the subsurface may fracture the caprock and lead to induced seismicity.

In order to explore the above mentioned risks and design GCS operations that minimize the risks, numerical modeling is often an essential tool. Considering that both CO_2 and brine are present, GCS is a multi-phase flow problem. Geomechanics and geochemistry may also be important to assess the risks, and therefore it may be necessary to solve the governing equations of multi-phase flow, geomechanics and geochemistry simultaneously, leading to very complex numerical models. Fortunately, several studies have found that for many GCS related problems the feedback of geochemistry and geomechanics on flow can be neglected (e.g., [3]), so that the multi-phase flow equations can be solved independently of geomechanics and geochemistry. Once the flow solution is known, geochemistry and geomechanics can be solved to study aspects such as species transport and induced seismicity. Most modeling studies related to GCS follow this approach of neglecting geochemistry and geomechanics, using reservoir simulators such as TOUGH2 [4], Eclipse [5] and MRST [6]. While these simplified three-dimensional models have lower data requirements and lower computational cost than the fully-coupled (flow + geochemistry + geomechanics) models, simplified three-dimensional simulations may still require tens of processors with execution times on the order of days. The solution approach can be further simplified by integrating the three-dimensional multi-phase flow equations in the vertical direction, leading to a set of two-dimensional multi-phase flow equations. For a more detailed description of modeling approaches used for GCS simulations the reader is referred to [7].

The goal of the study reported here is to investigate the applicability of vertically-integrated models for domains with vertical heterogeneity in intrinsic permeability, saturation – relative permeability relationships, and saturation – capillary pressure relationships. The heterogeneity patterns of interest here are not random, but follow patterns that are based on formations with a fluvial deposition history with coarser grained channels imbedded in a finer grained background. First, both the three-dimensional and vertically-integrated two-dimensional governing equations are described. Then, two test cases are introduced and results based on the two modeling approaches are compared. Lastly, conclusions based on those results are presented.

2. Modeling approaches

2.1. Three-dimensional governing equations

In the study presented here, the feedbacks of geomechanics and geochemistry are neglected, because the goal of the study is to investigate the applicability of vertically-integrated models to multi-phase flow in heterogeneous domains (i.e., neither geomechanics nor geochemistry have an impact). In addition, it is assumed that the two fluids are immiscible (i.e., no dissolution of CO_2 into brine or evaporation of water into CO_2) and that the system is isothermal. The migration of CO_2 and brine can thus be described by the three-dimensional governing equations of multi-phase flow. The conservation of mass for each phase are given by:

$$\frac{\partial}{\partial t}\left(\rho_\alpha \phi s_\alpha\right) + \nabla \cdot \left(\rho_\alpha \mathbf{u}_\alpha\right) = \psi_\alpha, \tag{1}$$

where ρ_α is the density of phase α [ML^{-3}], ϕ is the porosity [-], s_α is the saturation of phase α [-], ψ_α is the source/sink term [ML^{-3}T^{-1}], and α denotes the phase ($\alpha=c$ for super-critical CO$_2$; $\alpha=b$ for brine). The phase fluxes $\mathbf{u}_\alpha$ [LT^{-1}] are given by the multi-phase extension of Darcy's Law:

$$\mathbf{u}_\alpha = -\frac{k_{r,\alpha}\mathbf{k}}{\mu_\alpha}\left(\nabla p_\alpha - \rho_\alpha\mathbf{g}\right), \tag{2}$$

where $\mathbf{k}$ is the intrinsic permeability [L^2], $k_{r,\alpha}$ is the relative permeability of phase α [-], μ_α is the viscosity of phase α [ML^{-1}T^{-1}], p_α is the phase pressure [ML^{-1}T^{-2}], and $\mathbf{g}$ is the gravity acceleration vector [LT^{-2}]. The relative permeabilities and capillary pressure (p^{cap}) are assumed to be empirical functions of the brine saturation, so that

$$k_{r,\alpha} \equiv k_{r,\alpha}\left(s_b\right) \qquad\text{and}\qquad p_c - p_b \equiv p^{cap}\left(s_b\right) \tag{3}$$

This system of equations is closed by requiring that the entire pore space is occupied, so that

$$s_c + s_b = 1. \tag{4}$$

The system of equations given by equations (1) – (4) needs to be solved to simulate the migration of CO$_2$ and brine in the subsurface. Due to heterogeneous reservoir properties and non-linearities introduced by the relative permeability and capillary pressure relationships, the set of equations is commonly solved numerically, using approaches such as Implicit Pressure Explicit Saturation (IMPES) to deal with the non-linearity. Examples of reservoir simulators that solve this equation set are TOUGH2 [4], DuMuX [8], Eclipse [5] and MRST [6].

2.2. Vertically-integrated approach

The three-dimensional governing equations can be simplified by integrating in the direction perpendicular to the bedding plane of the formation of interest. As most formations are relatively close to horizontal, the integrated governing equations are usually termed vertically-integrated equations. Integrating over the thickness of the formation assumes that the impact of vertical flow can be neglected. This is usually a valid assumption in the GCS context, especially at later times, as the horizontal length scales are much larger than the thickness of the formation (i.,e., tens of kilometers compared to tens of meters) and because the large density difference between CO$_2$ and brine (on the order of 250-750 kg/m^3) leads to relatively fast vertical segregation of the two fluids. Integrating the conservation of mass equations for the two phases from the bottom of the formation (ξ_B) to the top of the formation (ξ_T) leads to:

$$\frac{\partial\left(\Phi S_\alpha\right)}{\partial t} + c_\alpha \Phi S_\alpha \frac{\partial P_\alpha}{\partial t} + \nabla \cdot \mathbf{U}_{\alpha,\|} = \Psi_\alpha, \tag{5}$$

where Φ is the integrated porosity [L], S_α is the depth averaged saturation of phase α [-], c_α is the linear compressibility coefficient of phase α [LT^{2}M^{-1}], P_α is the reference pressure of phase α (taken here as the pressure at the bottom of the formation) [ML^{-1}T^{-2}], $\mathbf{U}_{a,\|}$ are the vertically-integrated horizontal fluxes of phase α [L^{2}T^{-1}], and Ψ_α are integrated sources and sinks of phase α (including fluxes across the top and bottom of the formation) [LT^{-1}]. The integrated fluxes are given by

$$\mathbf{U}_{\alpha,\|} = -\mathbf{K}\Lambda_\alpha \cdot \left(\nabla_\| P_\alpha - \rho_\alpha \mathbf{G}\right), \tag{6}$$

where $\mathbf{K}$ is the vertically-integrated intrinsic permeability [L^3], Λ_α is an appropriately weighted vertically-averaged mobility of phase α [LTM^{-1}], the subscript $\|$ denotes a quantity/operator in the bedding plane, and $\mathbf{G} = \mathbf{e}_\| \cdot \mathbf{g} + \left(\mathbf{g}\cdot\mathbf{e}_3\right)\nabla_\|\xi_B$ with $\mathbf{e}_\| = \left(\mathbf{e}_1,\mathbf{e}_2\right)$. The other integrated quantities are defined by

$$S_\alpha = \frac{1}{\Phi}\int_{\xi_B}^{\xi_T}\phi s_\alpha dx_3, \quad \Phi = \int_{\xi_B}^{\xi_T}\phi dx_3, \quad \Psi_\alpha = \frac{1}{\rho_\alpha}\int_{\xi_B}^{\xi_T}\psi_\alpha dx_3, \quad \mathbf{K} = \int_{\xi_B}^{\xi_T}\mathbf{k}_\| dx_3, \quad \Lambda_\alpha = \mathbf{K}^{-1}\int_{\xi_B}^{\xi_T}\mathbf{k}_\|\frac{k_{r,\alpha}}{\mu_\alpha}dx_3. \tag{7}$$

The requirement that the entire pore space is filled by the two fluids can also be expressed by the depth-averaged saturations, so that

$$S_c + S_b = 1 \, . \tag{8}$$

The set of equations describing the migration of CO_2 and brine are now in terms of depth-averaged phase saturations (S_α) and reference pressure (P_α). However, the integrated phase mobilities (Λ_α) depend on the vertical profile of the phase saturation, and not on the depth-averaged saturation. This means that the saturation profiles need to be reconstructed based on the reference pressures and depth-averaged saturations. The profiles are usually reconstructed based on the assumption that CO_2 and brine segregate quickly compared to the overall modeling time scale. Once the fluids have segregated, there is no more vertical flow, which means that the pressure profiles of CO_2 and brine are hydrostatic (i.e., have a slope $\rho_\alpha g$). This assumption is called the vertical equilibrium assumption. The integrated mobilities can then calculated from algebraic equations based on these pressure profiles, the depth-averaged saturations and constitutive relations for capillary pressure and relative permeability (e.g., van Genuchten, Brooks-Corey). [9] introduced a reconstruction approach that does not rely on the vertical equilibrium assumption, but that reconstruction approach is not used here.

Vertically-integrated models have been used in several GCS related studies, but it is usually assumed that formations can either be represented as vertically-homogeneous layers or by a stack of layers, each of which is represented by a vertically-integrated model. In the study reported here, vertical heterogeneity in intrinsic permeability, relative permeability functions, and capillary pressure functions is taken into account by finding algebraic expressions for the integrated quantities shown in equation (7). The expressions can be derived using Brooks-Corey relationships for saturation, relative permeability and capillary pressure. The following form is used here

$$p^{cap} = p^{cap}_{entry} \left(s_{eff} \right)^{-1/\lambda} \, , \tag{9}$$

$$k_{r,b} = \left(s_{eff} \right)^{\frac{2+3\lambda}{\lambda}} \, , \tag{10}$$

$$k_{r,c} = \left(1 - s_{eff} \right)^2 \left[1 - \left(s_{eff} \right)^{\frac{2+\lambda}{\lambda}} \right] \, , \tag{11}$$

where p^{cap} is capillary pressure [$ML^{-1}T^{-2}$], p^{cap}_{entry} is capillary entry pressure [$ML^{-1}T^{-2}$], λ is the Brooks-Corey coefficient [-], and s_{eff} is the effective [-] defined by

$$s_{eff} = \frac{s_b - s_b^{res}}{1 - s_b^{res}} \, , \tag{12}$$

where s_b^{res} is the residual brine saturation.

3. Model description

In this study, CO_2 migration is simulated for two test cases consisting of channels with coarser material embedded in finer grained material using both a three-dimensional simulator and a vertically-integrated simulator. In the following, the coarser grained material is termed *sand* in reference to its initial deposition in a stream channel, while the finer grained material is termed *clay* as it was originally deposited in the floodplain. The TOUGH2/ECO2N simulator [4, 10] developed at Lawrence Berkeley National Lab is used for the three-dimensional models, while the VESA simulator developed at Princeton University is used for the vertically-integrated models.

All the test cases have a square model domain 5 km by 5 km in the horizontal and 50m in the vertical. The injection formation is horizontal (i.e., slope = 0), and CO_2 is injected into a single vertical well in the center of the domain. 1 Mt ($=10^9$ kg) is injected at a constant rate over a period of one year. The intrinsic permeabilities for the two facies are 200 mD and 1 mD for the sand and clay, respectively. Porosity for both facies is 0.2. Capillary entry pressure for the sand facies is 20 kPa and 200 kPa for the clay facies; the Brooks-Corey coefficient λ for both facies is 2. Unfortunately, Brook-Corey relationships are not implemented in TOUGH2, and therefore equivalent van Genuchten parameters were found to approximate the Brooks-Corey functions. Figure 1 and Figure 2 show the Brooks-Corey relative permeability and capillary pressure functions along with the equivalent van Genuchten functions.
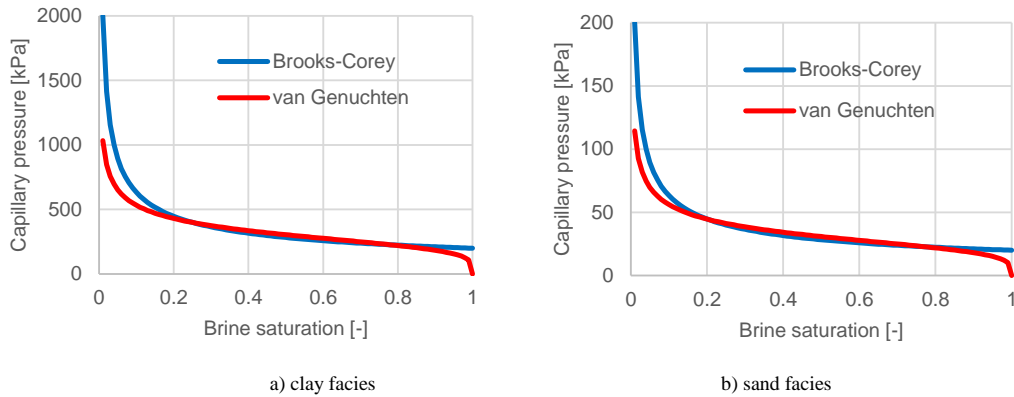
a) clay facies

b) sand facies

Figure 1: Capillary pressure functions for Brooks-Corey and van Genuchten for (a) sand facies and (b) clay facies
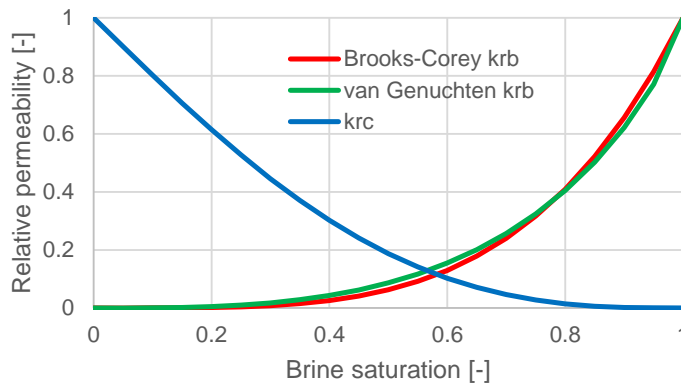

Figure 2: Relative permeability functions for Brooks-Corey and van Genuchten. Brooks-Corey and van Genuchten use the same formulation for relative permeability of CO_2. The relative permeability parameters are set to be same for the sand and clay facies.

Based on the depth-averaged brine saturation S_b defined in Equation (7) and the Brooks-Corey relationships described by Equations (9) – (11), integrated relative permeability functions can be derived. Figure 3 shows integrated permeability functions for four different vertical facies patterns: (a) clay for the entire column; (b) sand for the top 20m and clay for the bottom 30m; (c) clay for the top 15m, 20m of sand in the center, and clay again for the bottom 15m; (d) 30m of clay at the top and 20m sand at the bottom. Although the last three cases (b – d) have the same thickness of sand, the vertically-integrated relative permeability functions are different. This difference is due to the difference in where the majority of a fluid is: in the sand or in the clay facies. Figure 4 shows the reconstructed CO_2 profiles for the three facies patterns introduced above (b – d). For the case with sand at the top (b), the CO_2 saturation in the sand facies is high leading to a higher integrated relative permeability. For the case with the sand facies in the middle (c), the capillary pressure at the top of the formation is high enough to overcome the capillary entry pressure of the clay facies, so that some of the CO_2 is in the clay facies, leading to a lower integrated relative permeability. Even more CO_2 is in the clay facies for the case with sand at the bottom (d), leading to the lowest integrated relative permeability.
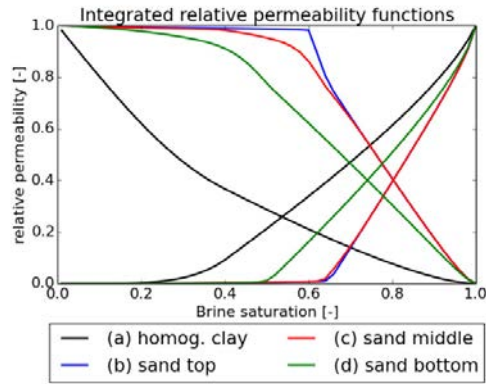
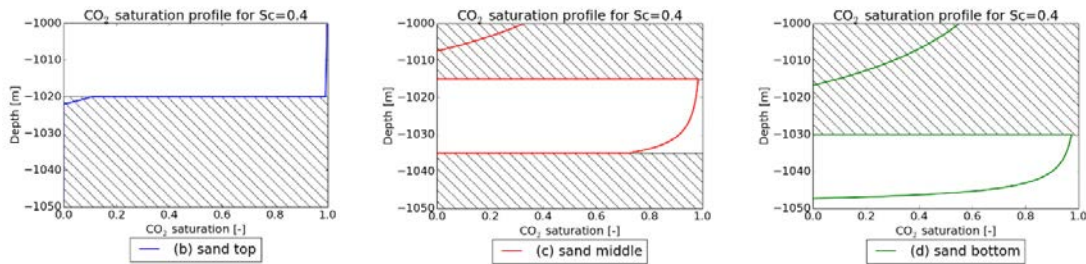Figure 3: integrated relative permeability functions for four cases

Figure 4: reconstructed CO_2 profiles

Two facies patterns are discussed in this paper. For the first pattern, the facies distribution is uniform in the horizontal, but heterogeneous in the vertical, leading to a model with horizontally continuous layers (termed the *layered model*). The second pattern consists of two intersecting sand facies channels in a clay facies background (termed the *channel model*). Both channels are 300m wide; one is parallel to the x-axis, the other is parallel to the y-axis. The channels span the entire model domain in their respective directions and intersect at the CO_2 injection location in the center of the domain. The thickness of the sand channels is 20m and their vertical location is in the middle of the formation. The two modeling approaches are compared based on the CO_2 plume after 1 year of injection. Plumes are compared based on the horizontal extent through plots of depth-averaged CO_2 saturation (S_c) and based on cross-sectional saturation profiles.

3.1. Layered model

The depth-averaged CO_2 plumes for the layered model show good agreement for the two modeling approaches (Figure 5). Both approaches predict radial plumes extending about 500m from the CO_2 injection well. While the plume predicted by the three-dimensional simulator is slightly larger, the overall shape and size of the plumes from the two simulators agree well with each other.
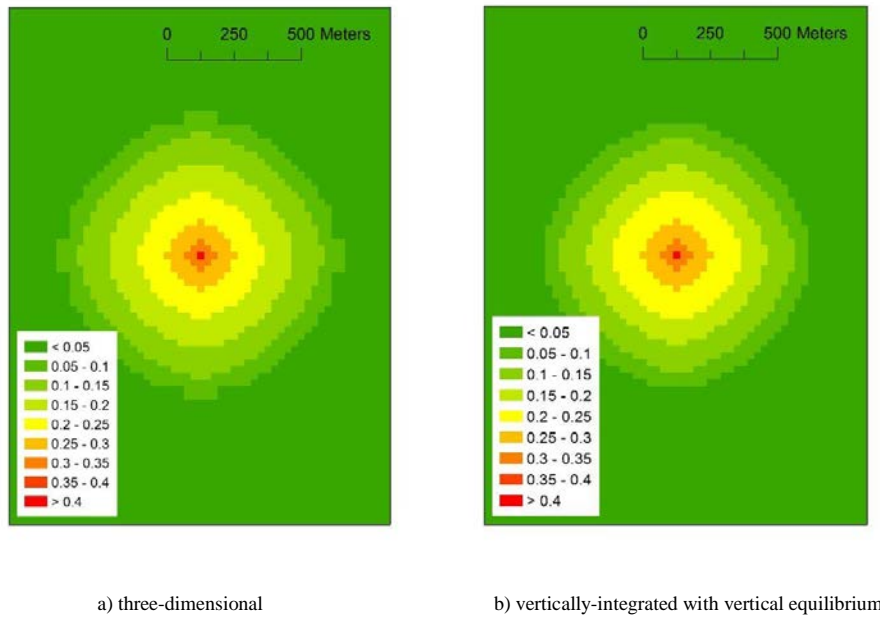
a) three-dimensional   b) vertically-integrated with vertical equilibrium

Figure 5: depth averaged CO_2 saturation after 1 year of injection for the layered model using the three-dimensional (a) and the vertically-integrated simulator (b).

Figure 6 shows CO_2 saturation profiles at the injection well for the layered model. The profiles are similar, with only very little CO_2 migrating into the clay facies, despite the vertical buoyancy drive. It should be pointed out, that the difference in capillary entry pressure (20 kPa in the sand facies, 200 kPa in the clay facies) is sufficient to keep CO_2 out of the clay facies even in a single-layer vertical-equilibrium model of the entire formation. A permeability contrast alone would not be sufficient, because the vertical permeability has no impact in a vertical equilibrium model. Therefore, much of the injected CO_2 would be predicted to reside in the upper clay facies; an unrealistic result. In addition, both approaches predict high CO_2 saturations close to the injection well. CO_2 saturation values are slightly higher at the upper part of the formation close to the injection well in the plume predicted by the three-dimensional simulator. However, the difference is minor and is likely due to the use of different relative permeability – saturation relationships (van Genuchten vs Brooks-Corey).
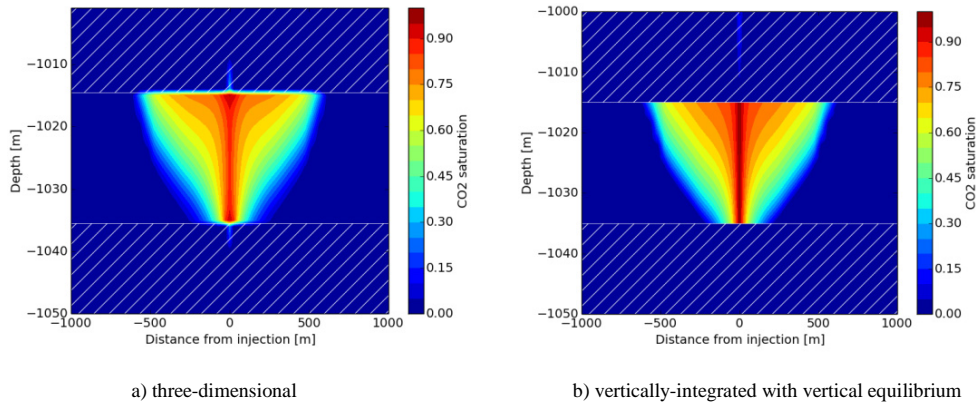
a) three-dimensional   b) vertically-integrated with vertical equilibrium

Figure 6: layered model CO_2 saturation profiles at injection well for the three-dimensional (a) and vertically-integrated (b) simulators. The white hatched areas show where the clay facies is present in the models.

3.2. Channel model

Figure 7 shows the depth-averaged CO_2 saturation after 1 year of constant injection for the channel model. The results from the two approaches agree well with each other, with plume tips reaching about 700m along the centers of the sand channels. The CO_2 plume predicted by the three-dimensional simulator gives a slightly more compact (i.e., higher saturation values close to the injection well). This is likely due to the use of slightly different relative permeability – saturation relationships. While not visible in the plots shown here, small amounts of CO_2 migrate into clay facies adjacent to the channels.
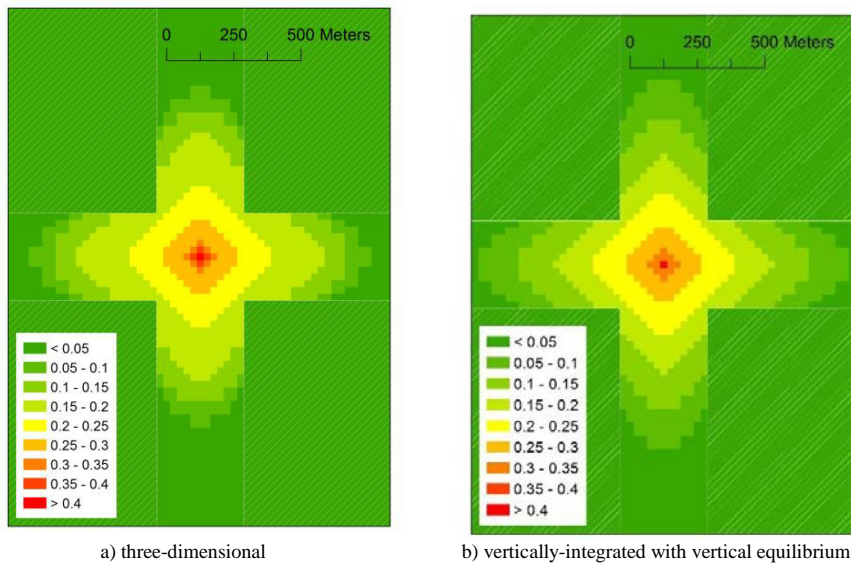

a) three-dimensional   b) vertically-integrated with vertical equilibrium

Figure 7: depth averaged CO_2 saturation after 1 year of injection for the channel model using the three-dimensional (a) and vertically-integrated (b) simulators. The white hatched areas show locations without embedded sand channels.

CO$_2$ saturation profiles for a cross-section perpendicular to the y-axis (i.e, in the x-z plane) and 175m from the injection well are given in Figure 8. The CO$_2$ stays confined in the sand facies channel, although a small amount of CO$_2$ appears in the clay facies adjacent to channel for the vertically-integrated simulator. This is unexpected as – based on the vertical equilibrium assumption - any CO$_2$ in the clay facies next to the channel should reside at the top of the formation, not close to the top of sand facies channel; further investigation is required to explain this artifact. Otherwise, the plume profiles compare well to each other, with the three-dimensional simulator having higher saturation in the upper part of the channel. Again, this is likely due to slightly different capillary pressure – saturation relationships used by the two simulators.
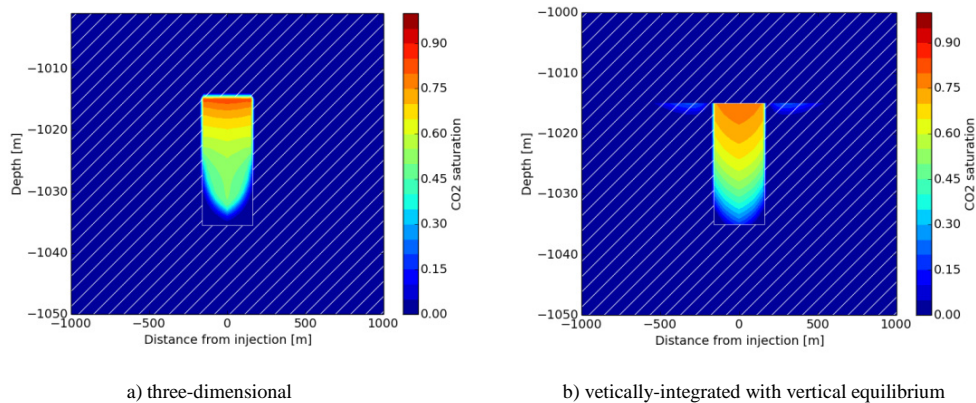

a) three-dimensional   b) vetically-integrated with vertical equilibrium

Figure 8: channel model CO$_2$ saturation profiles 175m from the injection well for the three-dimensional (a) and vertically-integrated (b) simulators. The white hatched areas show where the clay facies is present in the models.

4. Conclusion

In this article, we present an initial comparison of a vertically-integrated vertical equilibrium modeling approach with a three-dimensional modeling approach for CO$_2$ injection into heterogeneous domains. For the cases presented here, the heterogeneity consists of channels of coarser grained material (sand facies) embedded in a background of finer grained material (clay facies) as can be found in formations with fluvial deposition environments. The two facies have different intrinsic permeability, capillary pressure – saturation relationships and relative permeability – saturation relationships. The two modeling approaches are applied to two test cases: one consisting of a horizontally uniform layered system, with the sand facies sandwiched between two clay facies, and one with two intersecting sand facies channels imbedded in a clay background. The results show that both the depth-averaged CO$_2$ plumes and the cross-sectional CO$_2$ saturation profiles agree well with each other. The plume outlines predicted by the three-dimensional simulator tend to be slightly larger. The predicted cross-sectional CO$_2$ profiles show that both simulators predict that the CO$_2$ largely remains in the sand facies.

The results presented here are promising for the use of vertically-integrated vertical equilibrium simulators for the migration of CO$_2$ and brine in heterogeneous systems. It should be noted that using vertically-integrated modeling approaches comes with a significant reduction in computational effort. The three-dimensional simulations required 10 processors running for more than 24 hours, while the vertically-integrated simulations finished in a matter of hours on a single processor. More challenging conditions, such as lower permeability contrast and lower capillary entry pressure contrasts need to be investigated to determine the applicability of vertically-integrated vertical equilibrium models to the systems of interest here. It may also be necessary to use non-equilibrium vertically-integrated approaches such as those described by [9].

References

[1] Metz, B., et al., *International Panel on Climate Change Special Report on Carbon Dioxide Capture and Storage*. 2005, Cambridge: Cambridge University Press.
[2] Pacala, S. and R. Socolow, *Stabilization wedges: Solving the climate problem for the next 50 years with current technologies.* Science, 2004. **305**(5686): p. 968-972.
[3] Johnson, J.W., J.J. Nitao, and J.P. Morris, *Reactive Transport Modeling of Cap-Rock Integrity during Natural and Engineered Co2 Storage.* Carbon Dioxide Capture for Storage in Deep Geologic Formations - Results from the Co2 Capture Project, Vols 1 and 2, 2005: p. 787-813.
[4] Pruess, K., C.M. Oldenburg, and G. Moridis, *TOUGH2 user's guide.* 1999, Lawrence Berkeley National Laboratory, Berkeley, CA, USA.
[5] Schlumberger, *Eclipse Technnical Description*. 2010.
[6] Lie, K.A., et al., *Open-source MATLAB implementation of consistent discretisations on complex grids.* Computational Geosciences, 2012. **16**(2): p. 297-322.
[7] Bandilla, K.W., et al., *Multiphase Modeling of Geologic Carbon Sequestration in Saline Aquifers.* Groundwater, 2015. **53**(3): p. 362-377.
[8] Flemisch, B., et al., *DuMu(x): DUNE for multi-{phase, component, scale, physics, ...} flow and transport in porous media.* Advances in Water Resources, 2011. **34**(9): p. 1102-1112.
[9] Guo, B., et al., *Application of Vertically-Integrated Models with Subscale Vertical Dynamics to Field Sites for CO2 Sequestration.* 12th International Conference on Greenhouse Gas Control Technologies, Ghgt-12, 2014. **63**: p. 3523-3531.
[10] Pruess, K. and N. Spycher, *ECO2N - A fluid property module for the TOUGH2 code for studies of CO2 storage in saline aquifers.* Energy Conversion and Management, 2007. **48**(6): p. 1761-1767.